Dalton Transactions

ROYAL SOCIETY OF CHEMISTRY

PAPER

View Article Online
View Journal | View Issue

Open Access Article. Published on 22 May 2023. Downloaded on 1/22/2026 3:04:01 PM.
This article is licensed under a Creative Commons Attribution-NonCommercial 3.0 Unported Licence.

Check for updates

Cite this: *Dalton Trans.*, 2023, **52**, 8601

Why a simple vanadate is inefficient as a catalyst in the oxidation of alkanes with H_2O_2 – the long-standing puzzle is solved†‡

Maxim L. Kuznetsov * and Armando J. L. Pombeiro

Received 29th March 2023,
Accepted 18th May 2023

DOI: 10.1039/d3dt00967j

rsc.li/dalton

In contrast to V(v) complexes with various organic ligands, a simple vanadate without any additive is inactive in neutral medium toward the oxidation of alkanes with H_2O_2. In this work, we discovered that the insufficient activation of H_2O_2 upon coordination to the simple vanadate – the commonly accepted reason for the low catalytic activity of the vanadate – cannot explain this phenomenon. Two main findings are reported here on the basis of DFT calculations. First, the generally accepted Fenton-like mechanism of the generation of the active oxidizing species ($HO^{\bullet}$) in a vanadate/$H_2O_{2(aq)}$/MeCN system was revisited. A new mechanism based on the tremendous activation of the OOH ligand in the intermediate $[V(OO)_2(OOH)(H_2O)]$ toward the homolytic O–O bond cleavage is not only feasible but significantly more favourable than the Fenton-like pathway. The surprisingly low activation barrier calculated for the $HO^{\bullet}$ generation (15.4 kcal mol^{-1}) demonstrates the efficiency of this process. The presence of easily oxidizable non-innocent OO ligands in this intermediate explains such an activation. Second, it was found that the generated $HO^{\bullet}$ radicals may be easily captured by the V atom soon after their formation followed by the elimination of the molecular oxygen. This side reaction of the H_2O_2 dismutation efficiently consumes the produced $HO^{\bullet}$ radicals decreasing their concentration in the reaction mixture and preventing the following oxidation of alkanes.

Introduction

Alkanes represent a cheap and abundant carbon raw material, and their functionalization into various valuable organic products is of tremendous importance.[1–13] The main challenge associated with such transformations is the high chemical inertness of alkanes that requires the application of catalysts and strong oxidants. One of the most popular types of the catalysts used for the oxidation of alkanes is based on transition metal complexes or oxides. Vanadium is an element exhibiting several non-zero oxidation states, which permits its easy participation in various redox processes and enables broad applications of this element and its compounds in a number of catalytic reactions with the involvement of electron transfer (for reviews see ref. 13–33). Being the 6th most abundant transition metal on Earth, vanadium is quite cheap, and its usage as a catalyst is attractive from the economic point of view.

Several vanadium complexes with organic ligands (*e.g.* quinolin-8-olate, pyridine-2-carboxylate, triethanolaminate, bipyridines, phenanthrolines, terephthalohydrazides, NO_2-donor Schiff bases, *etc.*) demonstrated a high catalytic activity in the oxidation of alkanes with hydrogen peroxide.[34–38] Moreover, the simple vanadate VO_3^- was found to be active in these processes but only in the presence of either an appropriate additive (*e.g.* pyrazine-2-carboxylic acid, PCAH)[36,39] or a strong acid.[40] In the first case, the *in situ* formation of V-complexes with the additive occurs in solution, and these complexes serve as active catalytic forms. In the second case, the acidic medium provokes oligomerization of the vanadate, and the active catalytic form is divanadate.

The generally accepted Fenton-like mechanism includes (i) the formation of the H_2O_2 adduct with a catalyst molecule, (ii) proton transfer leading to a hydroperoxo intermediate, (iii) elimination of the $HOO^{\bullet}$ radical with the reduction of the vanadium atom to V(IV), (iv) formation of the second H_2O_2 adduct, (v) second H-transfer and (vi) elimination of the $HO^{\bullet}$ radical with the oxidation of the V(IV) atom[39] (Scheme 1). The formed $HO^{\bullet}$ radical directly oxidizes an alkane molecule *via* a hydrogen atom abstraction. The key feature of this mechanism is the direct participation of the metal centre in the electron transfer processes. At the $HOO^{\bullet}$ generation step, the V(v) atom

Centro de Química Estrutural, Institute of Molecular Sciences, Departamento de Engenharia Química, Instituto Superior Técnico, Universidade de Lisboa, Av. Rovisco Pais, 1049-001 Lisboa, Portugal. E-mail: max@mail.ist.utl.pt

† Dedicated to the memory of Prof. Georgiy B. Shul'pin.

‡ Electronic supplementary information (ESI) available. See DOI: https://doi.org/10.1039/d3dt00967j

Open Access Article. Published on 22 May 2023. Downloaded on 1/22/2026 3:04:01 PM.
This article is licensed under a Creative Commons Attribution-NonCommercial 3.0 Unported Licence.

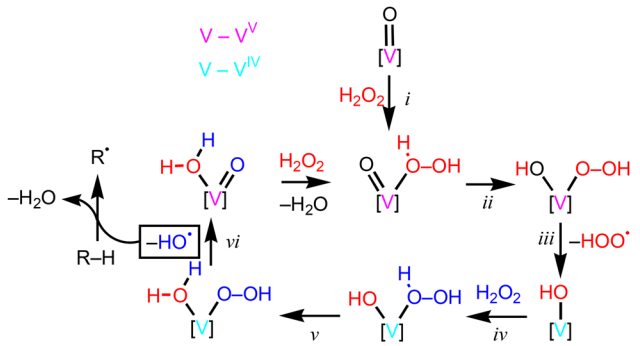

Scheme 1 Generally accepted mechanism of HO• formation from H_2O_2 catalysed by V(v) complexes.

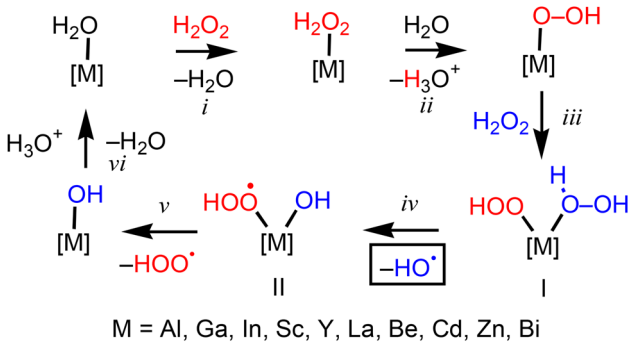

Scheme 2 Non-innocent ligand mechanism of HO• formation from H_2O_2 catalysed by salts of SSOS metals.

serves as an oxidant, while at the HO• formation step, the V(IV) centre is a reducing agent.

Meanwhile, the simple monomeric vanadate without any additive in the neutral medium – reaction conditions most attractive from the economic and environmental viewpoints – is not active toward the oxidation of alkanes with H_2O_2.[39,41] The commonly accepted reason is the insufficient activation of H_2O_2 by the vanadate toward HO• production that leads to a high activation barrier for this process. It is expected that the introduction of an appropriate organic ligand or a second vanadate unit (in the case of divanadate) into the vanadate molecule increases the potential of the catalyst to activate H_2O_2 and decreases the activation energy. However, to the best of our knowledge, this hypothesis was never proved either experimentally or theoretically.

Recently, the authors paid attention to the fact that inorganic salts of some metals bearing only a single stable non-zero oxidation state (SSOS metals such as Al, Ga, Zn, *etc.*) are quite active as catalysts for the oxidation of alkanes with H_2O_2.[42–44] The mechanism of a principally new type was proposed for these systems. This mechanism is based on the participation of a non-innocent (redox active) ligand in the catalyst molecule (or intermediate), whereas the metal oxidation state is not altered (the "non-innocent ligand mechanism"). It includes (i) the formation of a H_2O_2 adduct with the catalyst molecule, (ii) deprotonation of H_2O_2, (iii) addition of a second H_2O_2 molecule to give a key intermediate **I** bearing simultaneously the H_2O_2 and OOH^- ligands and (iv) homolytic HO–OH bond cleavage in the H_2O_2 molecule affording HO• and complex **II** with the hydroperoxyl radical ligand (Scheme 2). The OOH^- ligand in **I** is non-innocent and undergoes intramolecular oxidation upon HO–OH bond rupture. This oxidation stabilizes one of the products of the coordinated H_2O_2 decomposition and enables tremendous activation of H_2O_2 toward homolysis.

The non-innocent nature of the carbonate ligand and the hydrogen peroxide molecule in the Fenton like process between $[Co(H_2O)_6]^{2+}$ and H_2O_2 as well as the non-innocent character of the Cp ligand in the radical generation from the complexes $[Cp_2Ti(\eta^1\text{-}OO^tBu)L]$ (L = Cl^-, OTf^-, Br^-, OEt_2, Et_3P) were also previously reported.[45–48]

The initial goal of this study was two-fold, *i.e.* (i) to confirm (or disprove) that the HO• generation from H_2O_2 catalysed by the simple vanadate has a high activation barrier and, for this reason, this catalyst is not active and (ii) to verify if the non-innocent ligand mechanism may effectively operate also for catalysts with a metal exhibiting various oxidation states (such as vanadium) or if it is feasible only for the SSOS metals.

The results obtained demonstrated that the non-innocent ligand mechanism is not only feasible but more favourable than the conventionally accepted pathway, and the latter should be revisited. Another unexpected finding indicated that the low activity of the simple vanadate in this reaction is associated not with a high activation barrier of the HO• generation but with an efficient side reaction of H_2O_2 decomposition into O_2 and H_2O catalysed by vanadate. The results of this study are described and discussed below.

Computational details

The full geometry optimization of all structures and transition states (TS) has been carried out at the density functional theory (DFT) level using the PBE0 functional[49] with the atom-pairwise dispersion correction and the Becke–Johnson damping scheme D3BJ[50] with the help of the Gaussian-09 program package.[51] Recently, this functional demonstrated the excellent performance in the theoretical treatment of the activation of various main group bonds with (Ni,Pd)-based transition metal catalysts.[52] The geometry optimization was performed by using the aug-cc-pVDZ basis set for all atoms with consideration of the solvent effects applying the polarizable continuum model in the "solvent model of density" (SMD) version[53] with acetonitrile as the solvent typically used in the experimental studies of the alkane oxidation with H_2O_2 catalysed by V species.[34,36–40] Cartesian d and f basis functions (6d, 10f) were used in all calculations. No symmetry operations have been applied for any of the structures calculated. Singlet biradical structures were calculated using the broken symmetry approach[54–56] applied with the Guess = Mix Gaussian keyword.

This journal is © The Royal Society of Chemistry 2023

Open Access Article. Published on 22 May 2023. Downloaded on 1/22/2026 3:04:01 PM.
This article is licensed under a Creative Commons Attribution-NonCommercial 3.0 Unported Licence.

The Hessian matrix was calculated analytically for the optimized structures in order to prove the location of correct minima (no imaginary frequencies) or saddle points (only one imaginary frequency), and to estimate the thermodynamic parameters, the latter being calculated at a 298.15 K temperature and 1 atm pressure. The nature of all transition states was investigated by the analysis of vectors associated with the imaginary frequency and by the calculations of the intrinsic reaction coordinates (IRC) using the Gonzalez–Schlegel method.[57–59]

All possible geometrical isomers were calculated for all V complexes, and the most stable isomers are discussed (if not stated otherwise).

Results

In this section, first, equilibria in the vanadate/$H_2O_{2(aq)}$/MeCN catalytic system and the nature of the active catalytic species are discussed; second, the conventional mechanism of HO$^{\bullet}$ formation from H_2O_2 catalysed by the simple vanadate is analysed; third, the feasibility of the non-innocent ligand mechanisms is discussed; and fourth, the reasons for the low activity of the simple vanadate in the generation of the HO$^{\bullet}$ radicals are uncovered.

Equilibria in the vanadate/$H_2O_{2(aq)}$/MeCN system

Initial adducts. The reaction between the vanadate and hydrogen peroxide involves a series of H_2O_2 addition/substitution steps and proton transfers. In a solution bearing aqueous hydrogen peroxide, the coordination sphere of the vanadate HVO_3 may be saturated by water and/or H_2O_2 molecule(s). Equilibria between HVO_3 and the simple H_2O and/or H_2O_2 adducts are shown in Scheme 3. Among the aqua complexes, the most thermodynamically stable adduct is [V(=O)$_2$(OH)(H$_2$O)] (**1·H$_2$O**) with a tetrahedral arrangement of the ligands which contains one water molecule, while the octahedral complexes [V(=O)$_2$(OH)(H$_2$O)$_3$] (**1·3H$_2$O**) do not exist. In contrast, the most stable form of the H_2O_2 adduct is the trigonal bipyramid complex [V(=O)$_2$(OH)(H$_2$O$_2$)(H$_2$O)] (**1·H$_2$O$_2$·H$_2$O**) and this complex is the first reactive species toward the formation of the peroxo and diperoxo complexes of vanadium.

Formation of the monoperoxo complexes. Due to the acidic nature of the coordinated H_2O_2 in **1·H$_2$O$_2$·H$_2$O**, this molecule can lose a proton as a result of the intramolecular H-transfer either to one of the oxo-ligands to give [V(=O)(OH)$_2$(OOH)(H$_2$O)] (**2·H$_2$O**) or to the OH ligand affording [V(=O)$_2$(OOH)(H$_2$O)$_2$] (**3·2H$_2$O**) (Scheme 4). The latter pathway is slightly more kinetically favourable. The H-transfer occurs with the assistance of a water molecule which stabilizes the 6-membered transition states **TS1** and **TS2** (Fig. 1). The effect of water on the H-transfer in V-species has previously been discussed in detail.[36,40] For both channels, the following water liberation results in more stable tetrahedral complexes **2** and **3·H$_2$O**. Among all the mentioned hydroperoxo complexes, **2** is the most stable one and it is formed through the **1·H$_2$O$_2$·H$_2$O** → **3·2H$_2$O** → **3·H$_2$O** → **2** pathway. The second H-transfer in **2** from the OOH ligand either to the hydroxo or to the oxo ligand leads to the formation of the monoperoxo complex [V(=O)(OH)(OO)(H$_2$O)] (**4·H$_2$O**) or [V(OH)$_3$(OO)] (**5**), respectively. The first process is both kinetically and thermodynamically more feasible.

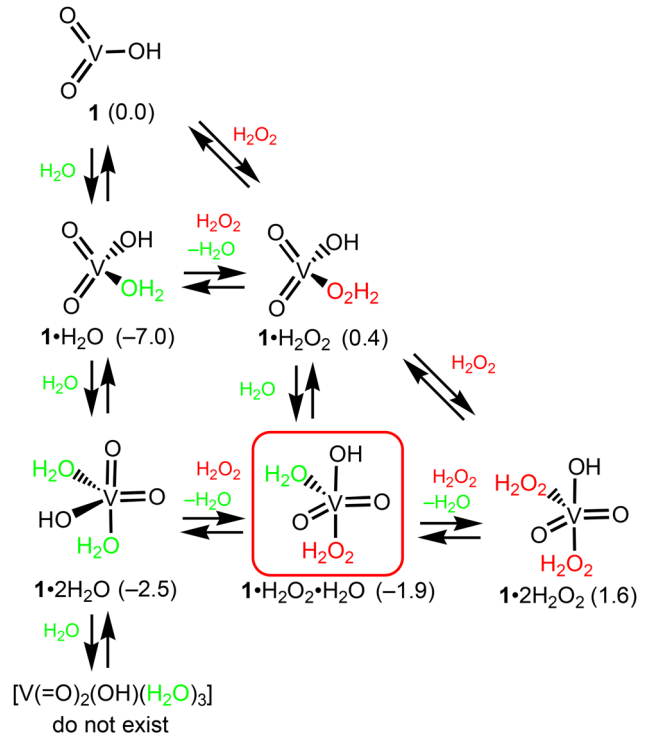

Scheme 3 Equilibria between HVO_3 and water or hydrogen peroxide adducts (Gibbs free energies are indicated in parentheses in kcal mol^{-1} relative to that of HVO_3, and the most stable H_2O_2 adduct is boxed; here and further, only the most stable geometrical isomers are shown).

Formation of the diperoxo complexes. This process starts with the associative substitution of H_2O for H_2O_2 in **4·H$_2$O** followed by the proton transfer which can occur to one of the =O, OH or OOH ligands in **4·H$_2$O$_2$** (Scheme 5). The calculations indicate that the most favourable route is the **4·H$_2$O** → **4·H$_2$O$_2$** → **7** → **6·H$_2$O** one. The second H-transfer affords the diperoxo species [V(OH)(OO)$_2$(H$_2$O) (**9·H$_2$O**). Finally, one more substitution of H_2O for H_2O_2 in **9·H$_2$O** and the proton transfer yield the hydroperoxo diperoxo complex [V(OOH)(OO)$_2$(H$_2$O)] (**10·H$_2$O**). The last two species are the most thermodynamically stable ones in the vanadate/$H_2O_{2(aq)}$/MeCN system. The discussed equilibria are easily established, and the activation barriers for the formation of the most stable intermediates do not exceed 12.4 kcal mol^{-1}.

Conventional Fenton-like mechanism of HO$^{\bullet}$ generation

The general scheme of the currently accepted Fenton-like mechanism of HO$^{\bullet}$ radical formation from H_2O_2 catalysed by a V(v) species was discussed in Introduction and it is shown in

Open Access Article. Published on 22 May 2023. Downloaded on 1/22/2026 3:04:01 PM.
This article is licensed under a Creative Commons Attribution-NonCommercial 3.0 Unported Licence.

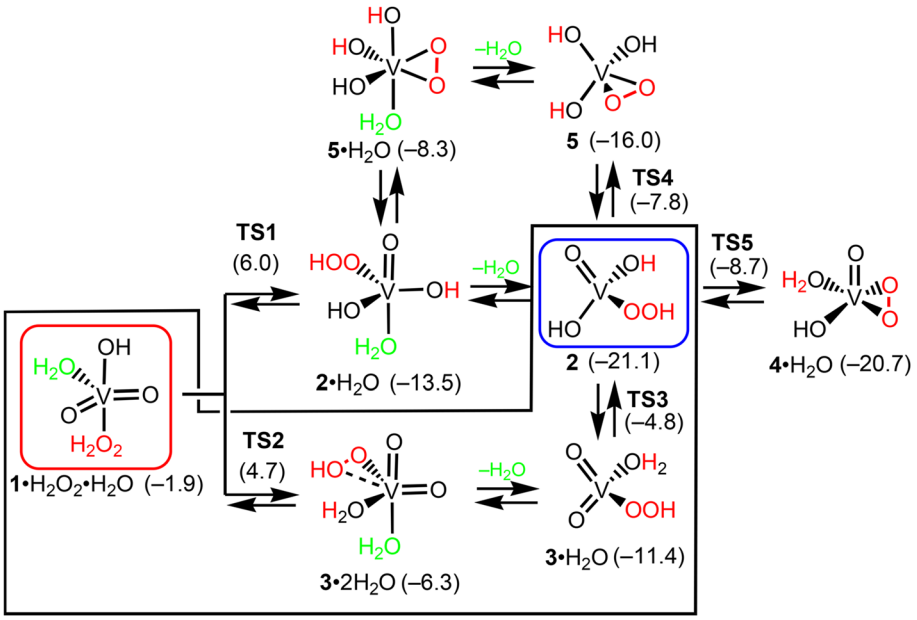

Scheme 4 Mechanisms of the formation of monoperoxo complexes (Gibbs free energies are indicated in parentheses in kcal mol^{-1} relative to that of HVO_3; the initial and final species of this step and the most plausible pathway are indicated).

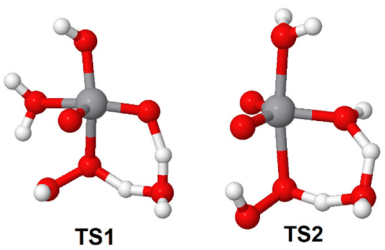

Fig. 1 Equilibrium structures of **TS1** and **TS2**.

Scheme 1. The active catalytic forms in the vanadate/$H_2O_{2(aq)}$/MeCN system, which initiate this mechanism, are the V(v) hydroperoxo complexes **2**, **6·H₂O** and **10·H₂O**.

The HOO˙ formation step. Elimination of the HOO˙ radical from the hydroperoxo species upon V–OOH bond cleavage affords the reduced V(IV) complexes $[V(=O)(OH)_2(H_2O)_2]$ (**11·2H₂O**), $[V(=O)(OO)(H_2O)_2]$ (**12·2H₂O**) and $[V(OO)_2(H_2O)]$ (**13·H₂O**) (Scheme 6). In the case of complexes **2** and **6·H₂O**, this process occurs *via* an associative mode including initial addition of two or one H_2O molecules, respectively, and the

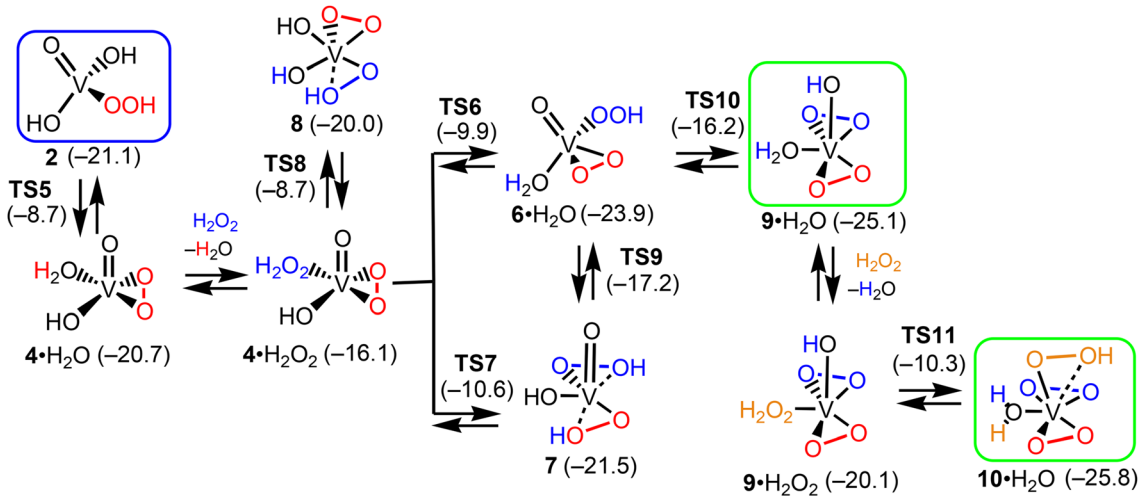

Scheme 5 Mechanisms of the formation of diperoxo complexes (Gibbs free energies are indicated in parentheses in kcal mol^{-1} relative to that of HVO_3; the initial species of this step and the most stable complexes in the vanadate/$H_2O_{2(aq)}$/MeCN system are boxed).

This journal is © The Royal Society of Chemistry 2023

Open Access Article. Published on 22 May 2023. Downloaded on 1/22/2026 3:04:01 PM.
This article is licensed under a Creative Commons Attribution-NonCommercial 3.0 Unported Licence.

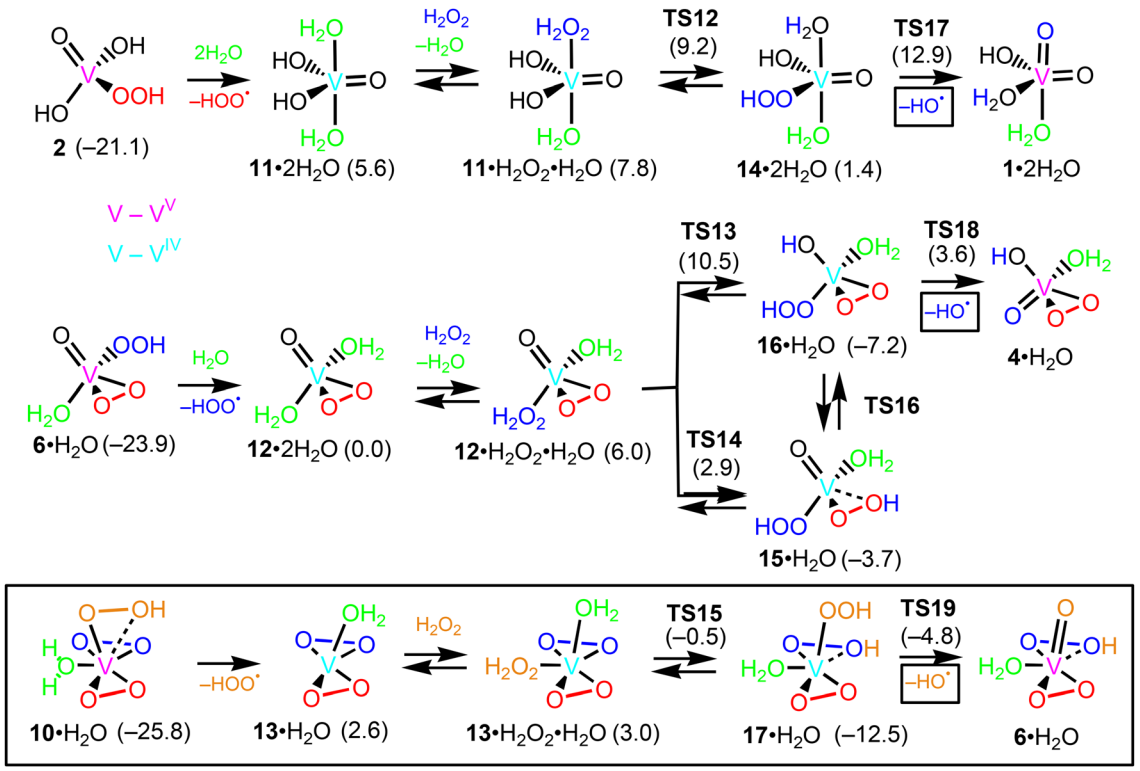

Scheme 6 Conventional mechanisms of HO˙ generation (Gibbs free energies are indicated in parentheses in kcal mol^{-1} relative to that of HVO_3, and the most favourable pathway is boxed).

following HOO˙ elimination (Scheme S1 in the ESI‡). In the case of complex **10·H$_2$O**, the HOO˙ generation is realized dissociatively. The V–OOH bond cleavage is accompanied by the monotonous increase of the total energy of the system. The potential energy surface (PES) scan in **6·H$_2$O** indicates that until a V–OOH distance of *ca.* 2.41 Å is achieved, the singlet closed shell configuration is the most stable one (Fig. 2, left). At a longer distance, the singlet biradical configuration with unpaired electrons localized at the V atom and the leaving OOH group becomes more stable (Fig. 2, right).

The HO˙ formation step. At this step, the hydrogen peroxide adducts [V(=O)(OH)$_2$(H$_2$O$_2$)(H$_2$O)] (**11·H$_2$O$_2$·H$_2$O**), [V(=O)(OO)(H$_2$O$_2$)(H$_2$O)] (**12·H$_2$O$_2$·H$_2$O**) and [V(OO)$_2$(H$_2$O$_2$)(H$_2$O) (**13·H$_2$O$_2$·H$_2$O**) are formed upon water substitution for H$_2$O$_2$ or addition of H$_2$O$_2$ (Scheme 6). The subsequent proton transfer from the coordinated H$_2$O$_2$ molecule can occur to the oxo, hydroxo or peroxo ligand furnishing the hydroperoxo V(IV) complexes [V(=O)(OH)(OOH)(H$_2$O)$_2$] (**14·2H$_2$O**), [V(OH)(OOH)(OO)(H$_2$O)] (**16·H$_2$O**) and [V(OOH)$_2$(OO)(H$_2$O) (**17·H$_2$O**). The formation of **16·H$_2$O** occurs in two steps *via* complex **15·H$_2$O**. Finally, the O–O bond cleavage in the OOH ligand yields the HO˙ radical and restores the V(V) active catalytic forms.

The non-innocent ligand mechanisms of HO˙ generation

In this mechanism, the HO˙ radical is formed either from the OOH ligand in a V(V) complex or from the coordinated H$_2$O$_2$ molecule which are activated toward the O–O homolysis due to the presence of a non-innocent ligand in the complex.

Homolysis of the OOH ligand in the V(V) complexes. As discussed above, the establishing of the equilibria in the vanadate/H$_2$O$_{2(aq)}$/MeCN system leads to the formation of three stable hydroperoxo V(V) complexes, *i.e.* [V(=O)(OH)$_2$(OOH)] (**2**), [V(=O)(OOH)(OO)(H$_2$O)] (**6·H$_2$O**) and [V(OOH)(OO)$_2$(H$_2$O)] (**10·H$_2$O**).

Thermodynamic consideration. The dissociation of the OOH ligand in the first complex produces HO˙ and [V(O)$_2$(OH)$_2$] (**18**) but it is endergonic by 35.9 kcal mol^{-1} (Scheme 7). Such a high value is not surprising given that there is no non-innocent ligand in **2**. This value is only by 2.0 kcal mol^{-1} lower than that for the homolytic dissociation of free H$_2$O$_2$ (37.9 kcal mol^{-1}).

A qualitatively different situation was found for the OOH homolyses in **6·H$_2$O** and **10·H$_2$O**. In the former species, the ΔG° value of HO˙ formation is only +5.8 kcal mol^{-1}, whereas in the latter complex, this process is *exergonic* by –8.2 kcal mol^{-1} indicating that the generation of HO˙ from **10·H$_2$O** is thermodynamically spontaneous. The reasons of such huge thermodynamic activation of OOH in these complexes become clear from the analysis of the products of this step, [V(O)$_2$(OO)(H$_2$O)] (**19·H$_2$O**) and [V(O)(OO)$_2$(H$_2$O)] (**20·H$_2$O**). The unpaired electron in these doublet species is localized at the OO ligand rather than at the V atom (Fig. 3). Thus, the HO˙ elimination does not result in a change of the V oxidation state which remains at +5. The

Open Access Article. Published on 22 May 2023. Downloaded on 1/22/2026 3:04:01 PM.
This article is licensed under a Creative Commons Attribution-NonCommercial 3.0 Unported Licence.

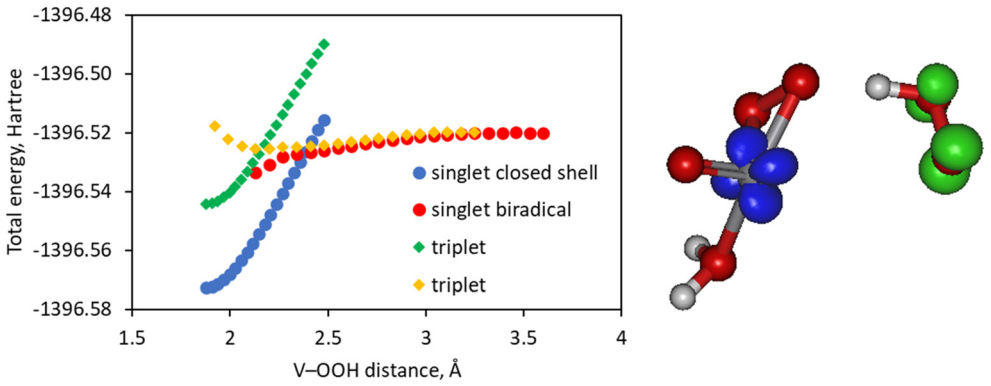

Fig. 2 PES scans for the elongation of the V–OOH bond in the complex **6·H$_2$O** (left, scans of two electronic triplet configurations are indicated) and a plot of spin density for the singlet biradical structure at a V–OOH distance of 3.6 Å (right).

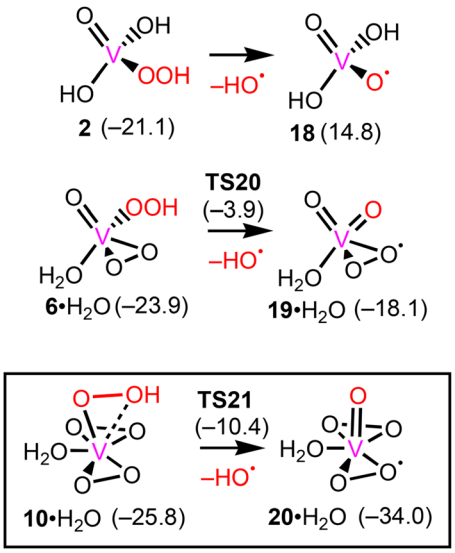

Scheme 7 Formation of the HO$^\bullet$ radical from the hydroperoxo V(v) complexes through the non-innocent ligand mechanism (Gibbs free energies are indicated in parentheses in kcal mol^{-1} relative to that of HVO_3, and the most favourable pathway is boxed).

homolytic VO–OH bond cleavage produces a free HO$^\bullet$ radical and an oxyl anion-radical O$^{\bullet-}$ which is coordinated to V in **19·H$_2$O** or **20·H$_2$O**. During the O–O bond rupture, the coordinated O$^{\bullet-}$ anion-radical is reduced intramolecularly, oxidizing the OO ligand and not the V centre as in the V(IV) complexes **11·2H$_2$O**, **12·2H$_2$O** and **13·H$_2$O** of the conventional mechanism. As a result, O$^{\bullet-}$ is transformed into the oxo ligand $(=O)^{2-}$, while the peroxo $(OO)^{2-}$ ligand is oxidized into the peroxyl species $(OO)^{\bullet-}$. Therefore, the $(OO)^{2-}$ ligand exhibits non-innocent behaviour which permits further oxidation of the V(v) complexes **6·H$_2$O** and **10·H$_2$O** despite them bearing the metal centre in its highest oxidation state. The ability of the $(OO)^{2-}$ ligand to be easily oxidized is a driving force for the tremendous thermodynamic activation of OOH in the hydroperoxo V(v) complexes **6·H$_2$O** and **10·H$_2$O**.

Kinetic consideration. The low ΔG° values of HO$^\bullet$ formation from **6·H$_2$O** and **10·H$_2$O** allow the assumption that these processes are controlled by kinetic factors rather than by thermodynamic ones. The analysis of the kinetic features is not trivial in this case since the initial complexes are singlet close shell structures while both reaction products are doublets. Therefore, the PES scans for the VO–OH bond cleavage in **6·H$_2$O** and **10·H$_2$O** at different spin states were firstly analysed. At the singlet close shell PES, an increase of the VO–OH distance corresponding to the heterolytic VO–OH bond cleavage is accompanied by the monotonic enhancement of the system's energy (Fig. 4). This process is unfavourable, and the elongation of the VO–OH bond until 2 Å requires 30–33 kcal mol^{-1}.

The adiabatic excitation of **6·H$_2$O** with the unrelaxed VO–OH bond distance to the singlet biradical state ^{1,1}**6·H$_2$O** requires only 12.2 kcal mol^{-1}. One of the unpaired electrons in ^{1,1}**6·H$_2$O** is localized at the V atom while another one is mostly distributed among the peroxo ligand (Fig. 4A). The OOH

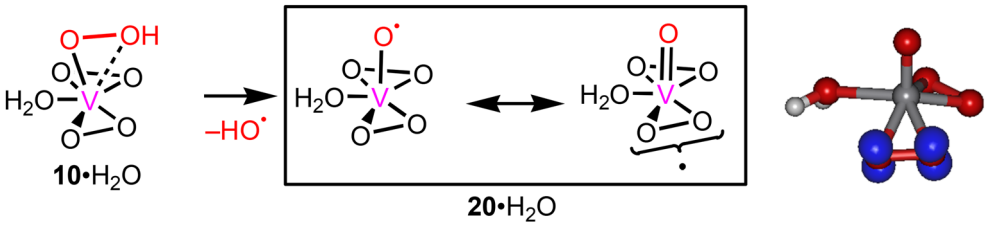

Fig. 3 O–OH bond cleavage in **10·H$_2$O**, intramolecular electron transfer and spin density distribution in **20·H$_2$O**.

This journal is © The Royal Society of Chemistry 2023

Open Access Article. Published on 22 May 2023. Downloaded on 1/22/2026 3:04:01 PM.
This article is licensed under a Creative Commons Attribution-NonCommercial 3.0 Unported Licence.

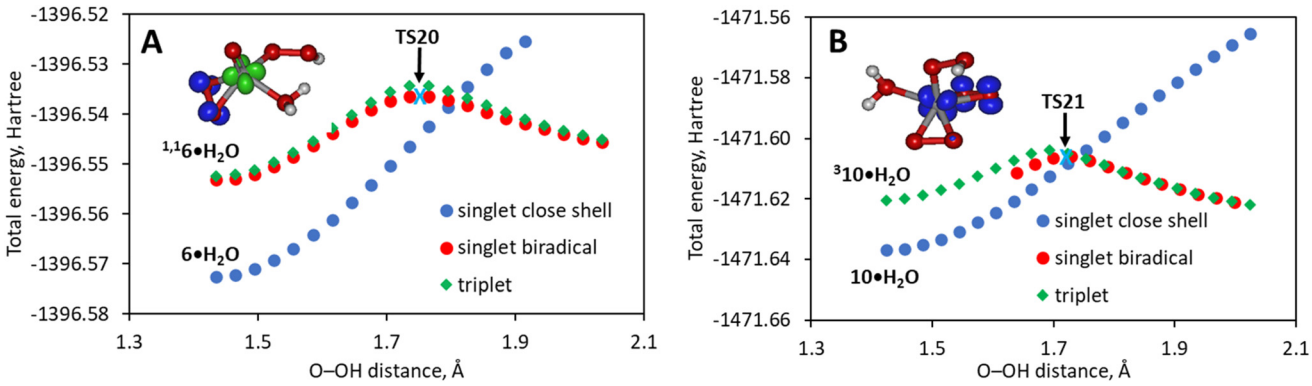

Fig. 4 PES scans for the elongation of the VO–OH bond in complexes **6·H$_2$O** (A) and **10·H$_2$O** (B) (positions of the equilibrium structures of **TS20** and **TS21** are shown by cross and plots of spin density for ^{1,1}**6·H$_2$O** and ^{3}**10·H$_2$O** are provided).

ligand being bidentate in the ground state of **6·H$_2$O** becomes monodentate in ^{1,1}**6·H$_2$O**. The V–O$_{(OO)}$ bonds elongate upon excitation from 1.82–1.83 Å to 1.96–1.99 Å which corresponds to the formation of the peroxyl ligand $(OO)^{\bullet-}$. Thus, this excitation results in the formation of a V(IV) species due to an intramolecular redox process between the metal centre and the OO ligand. Upon increase of the VO–OH distance, the total energy on the singlet biradical PES reaches the maximum at 1.74 Å and then decreases.

The PES character of the complex **10·H$_2$O** is similar (Fig. 4B). In this case, the singlet biradical structures could be calculated only for VO–OH distances longer than 1.63 Å. The initial excitation energy to the triplet state ^{3}**10·H$_2$O** is 10.4 kcal mol^{-1}. The excitation affects only one peroxo ligand.

With the help of PES scan results, the singlet biradical transition states **TS20** and **TS21** which correspond to the homolytic VO–OH bond cleavage in **6·H$_2$O** and **10·H$_2$O** were located (Fig. 5). The spin density in these TSs is mostly localized at the V atom ($\rho_{s,\alpha}$ = 0.81 and 0.72*e*), one OO ligand ($\rho_{s,\beta}$ = 1.05*e*) and the oxygen atom of the leaving HO$^{\bullet}$ radical ($\rho_{s,\alpha}$ = 0.54 and 0.53*e*). Thus, the VO–OH bond rupture in the excited complexes ^{1,1}**6·H$_2$O** and ^{1,1}**10·H$_2$O** leads to the intramolecular reduction of the oxygen atom coordinated to the V atom to form the oxo ligand O^{2-}.

Homolysis of the coordinated H$_2$O$_2$. Coordination of H$_2$O$_2$ to the V(V) centre can activate this molecule toward homolysis and formation of the HO$^{\bullet}$ radical (Scheme 8). Three H$_2$O$_2$ adducts can be formed in the vanadate/H$_2$O$_{2(aq)}$/MeCN system, *i.e.* [V(=O)$_2$(OH)(H$_2$O$_2$)(H$_2$O)] (**1·H$_2$O$_2$·H$_2$O**), [V(=O)(OH)(OO)(H$_2$O$_2$)] (**4·H$_2$O$_2$**) and [V(OH)(OO)$_2$(H$_2$O$_2$)] (**9·H$_2$O$_2$**). The decomposition of **1·H$_2$O$_2$·H$_2$O** into HO$^{\bullet}$ and [V(=O)$_2$(OH)$_2$(H$_2$O)] (**21·H$_2$O**) is not favourable due to the absence of any non-innocent ligands in this complex (ΔG° = 25.3 kcal mol^{-1}). In contrast, the homolysis of H$_2$O$_2$ in the other two adducts is exergonic by −9.7 and −2.1 kcal mol^{-1} because of the presence of the redox active peroxo ligand. As in the case of the V(V) hydroperoxo species, the homolytic HO–OH bond cleavage in **4·H$_2$O$_2$** and **9·H$_2$O$_2$** results in the intramolecular oxidation of the redox active OO ligand to the $OO^{\bullet-}$ anion-radical and reduction of the formed coordinated OH group, while the oxidation state of vanadium remains intact.

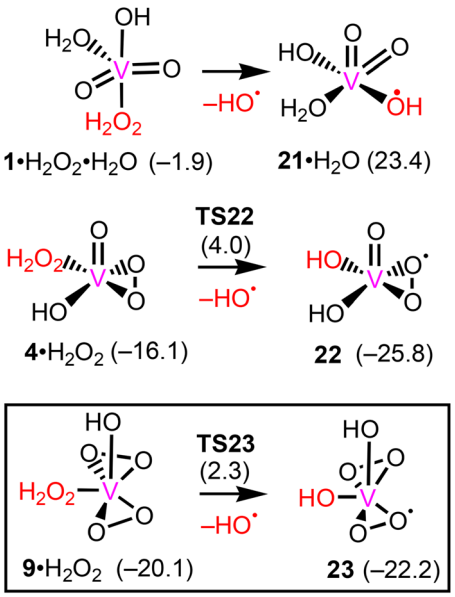

Scheme 8 Formation of the HO$^{\bullet}$ radical from the hydrogen peroxide V(V) complexes through the non-innocent ligand mechanism (Gibbs free energies are indicated in parentheses in kcal mol^{-1} relative to that of HVO_3, and the most favourable pathway is boxed).

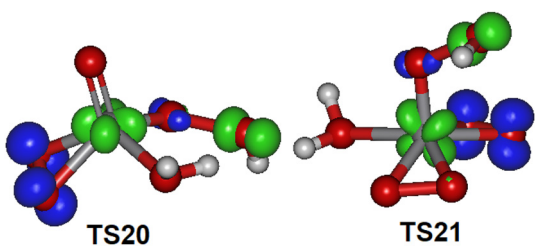

Fig. 5 Equilibrium structures and plots of spin densities for **TS20** and **TS21**.

Open Access Article. Published on 22 May 2023. Downloaded on 1/22/2026 3:04:01 PM.
This article is licensed under a Creative Commons Attribution-NonCommercial 3.0 Unported Licence.

The PES scan analysis allowed the localization of the singlet biradical transition states **TS22** and **TS23** corresponding to the homolytic HO–OH bond cleavage in **4·H$_2$O$_2$** and **9·H$_2$O$_2$** (Fig. S1 in ESI‡). The spin density in **TS22** and **TS23** is mostly localized at the V atom, one peroxo ligand and the leaving HO$^\bullet$ radical.

Activation energies and comparison of reaction mechanisms

The inspection of the calculated mechanisms indicates the following. First, in the solution of vanadate with aqueous hydrogen peroxide, several diperoxo, monoperoxo and hydroperoxo complexes are easily formed. The diperoxo complexes **9·H$_2$O** and **10·H$_2$O** are the most thermodynamically stable in such a solution, and they are in equilibrium with other slightly less stable monoperoxo and hydroperoxo complexes **6·H$_2$O**, **7**, **4·H$_2$O** and **2** (Scheme 5). The diperoxo and monoperoxo V(v) species were detected experimentally in the aqueous solution in the presence of H_2O_2 using the NMR technique.[60–63]

Second, the most favourable pathway of the conventional mechanism is based on the hydroperoxo diperoxo complex **10·H$_2$O** and includes the sequence of steps **10·H$_2$O** → **13·H$_2$O** (+HOO$^\bullet$) → **13·H$_2$O$_2$·H$_2$O** → **17·H$_2$O** → **6·H$_2$O** (+HO$^\bullet$) (Scheme 6). The overall Gibbs free energy of activation for HO$^\bullet$ formation in this pathway is 28.8 kcal mol^{-1} relative to **10·H$_2$O**. The rate determining step is the formation of the V(IV) hydrogen peroxide adduct **13·H$_2$O$_2$·H$_2$O**.

Third, the non-innocent ligand mechanism based on the simple homolysis of the OOH ligand in [V(OOH)(OO)$_2$(H$_2$O)] **10·H$_2$O** (Scheme 7) is significantly more favourable than the conventional mechanism. This pathway has an activation barrier of 15.4 kcal mol^{-1} relative to **10·H$_2$O**, and the rate limiting step is the VO–OH bond cleavage in **10·H$_2$O**.

Fourth, the non-innocent ligand mechanism based on the homolysis of H_2O_2 coordinated in [V(OH)(OO)$_2$(H$_2$O$_2$)] **9·H$_2$O$_2$** has an activation energy of 28.1 kcal mol^{-1} relative to **10·H$_2$O** which is comparable to that of the conventional mechanism (Scheme 8).

Fifth, the presence of two peroxo ligands in the catalytic complexes is crucial for the highest activation of the H_2O_2 and OOH ligands toward homolysis. All pathways based on the monoperoxo species **2** and **6·H$_2$O** require a higher activation barrier than the pathways of the same mechanism based on the diperoxo complex **10·H$_2$O**.

Thus, one of the most important results of this work is that *the mechanism involving the non-innocent peroxo ligand is not only feasible but also more favourable than the conventional Fenton-like mechanism*.

Why a simple vanadate is not efficient as a catalyst for the oxidation of alkanes with H_2O_2?

The calculated overall activation barrier for the most plausible mechanism of HO$^\bullet$ generation is 15.4 and 17.4 kcal mol^{-1} in terms of the Gibbs free energy and enthalpy of activation, respectively. Such low values make the generation of the HO$^\bullet$ radicals in the vanadate/$H_2O_{2(aq)}$/MeCN system quite efficient. The latter value correlates well with the experimental activation energy of HO$^\bullet$ generation in the *n*-Bu$_4$NVO$_3$/PCAH/$H_2O_{2(aq)}$/MeCN system which is active for the oxidation of alkanes (17 ± 2 kcal mol^{-1} (ref. 39)). *Thus, the low activity of the simple vanadate (without any additive) as a catalyst in the oxidation of alkanes with H_2O_2 cannot be justified by the high activation energy for this process.*

During the search for PES for the VO–OH bond cleavage in **10·H$_2$O** it was found that the liberating HO$^\bullet$ radical can easily be trapped by the V atom soon after the formation of **TS21**. Indeed, the PES scan for the shortening of the V···OH$_{leaving}$ distance starting from a point on the energy curve after **TS21** revealed a barrier of HO$^\bullet$ capture of only 2.0 kcal mol^{-1} (Fig. 6, see the ESI‡ for details). As a result, the singlet biradical complex [V(=O)(OH)(OO)$_2$] (^{1,1}**24**) is formed that is accompanied by an extrusion of the water molecule initially coordinated in **10·H$_2$O**. The spin density in ^{1,1}**24** is localized at two peroxo OO ligands (1.07*e* for each ligand, Fig. 7) which

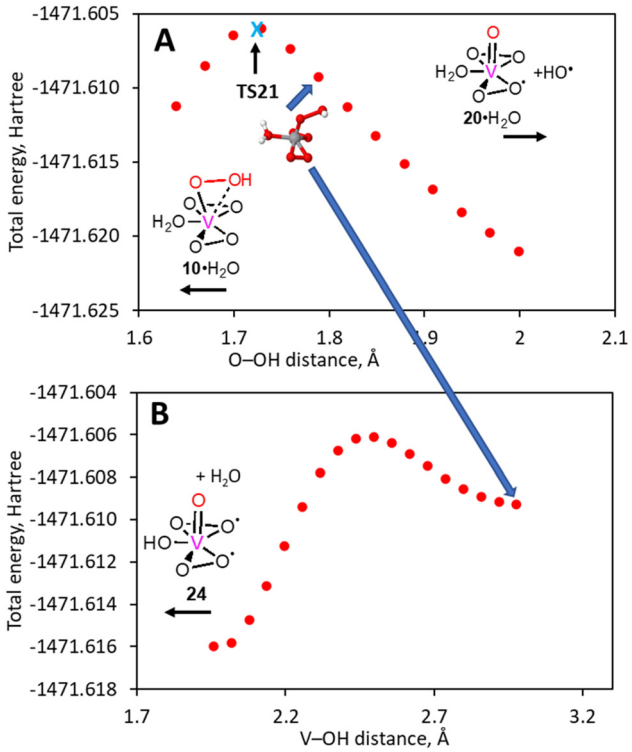

Fig. 6 Singlet biradical PES scans for the O–OH bond cleavage in **10·H$_2$O** (A) and for the shortening of the V···OH$_{leaving}$ distance from one of the points on the reaction path after **TS21** (B).

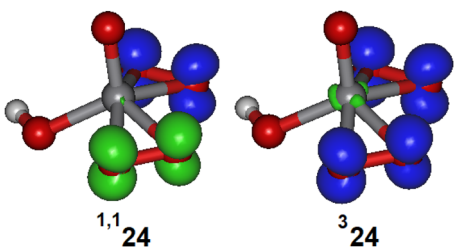

Fig. 7 Plots of spin density in ^{1,1}**24** and ^{3}**24**.

This journal is © The Royal Society of Chemistry 2023

Open Access Article. Published on 22 May 2023. Downloaded on 1/22/2026 3:04:01 PM.
This article is licensed under a Creative Commons Attribution-NonCommercial 3.0 Unported Licence.

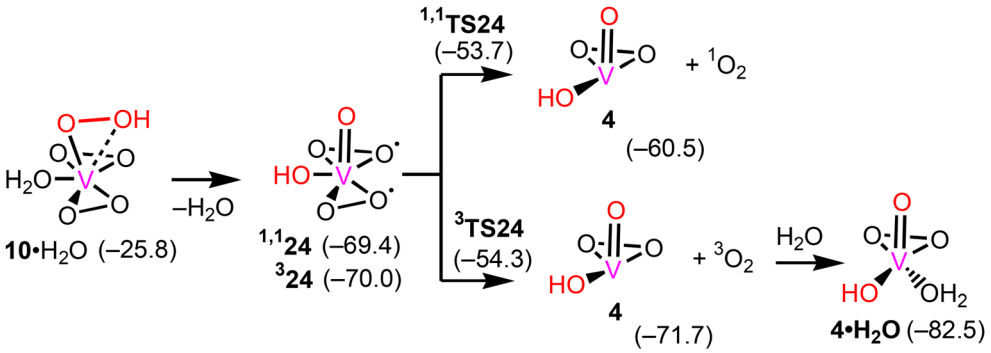

Scheme 9 HO$^{\bullet}$ radical trap upon O–OH bond cleavage in **10·H$_2$O** and the following liberation of O_2.

corresponds to the structure with two anion-radical peroxyl ligands $(OO)^{\bullet-}$. The spin conversion from the singlet biradical to the triplet state ^{3}**24** then occurs, the latter state being more stable by 0.6 kcal mol^{-1}. Both states have similar spin distribution with some involvement of the V atom in the case of the triplet structure.

The formation of complex **24** from **10·H$_2$O** is highly exergonic by (–43.6)–(–44.2) kcal mol^{-1} (Scheme 9). Both singlet biradical and triplet complexes **24** can easily lose the molecular oxygen affording the monoperoxo species [V(=O)(OH)(OO)] (**4**) which is stabilized by water addition to give **4·H$_2$O**. The singlet biradical channel leads to the formation of the singlet oxygen which was detected experimentally in the reactions of the V(v) species with H_2O_2.[64] Upon these processes, one of the $(OO)^{\bullet-}$ ligands experiences further oxidation to O_2, whereas another $(OO)^{\bullet-}$ ligand is reduced to the peroxo ligand $(OO)^{2-}$ (Fig. 8). The O_2 liberation has quite a low activation barrier of 15.7 kcal mol^{-1} and it is exergonic by –12.5 kcal mol^{-1}. Thus, the HO$^{\bullet}$ radical trapping by the V centre is very efficient. Overall, this reaction channel corresponds to the catalytic dismutation of H_2O_2 into O_2 and H_2O (Scheme 10). The consumption of HO$^{\bullet}$ in this side reaction significantly decreases the concentration of these radicals in the reaction mixture and makes their interaction with an alkane molecule inefficient.

Discussion and final remarks

The low efficiency of the simple vanadate as a catalyst in the homogeneous oxidation of alkanes with H_2O_2 is a long-standing puzzle. Insufficient activation of H_2O_2 toward the production of HO$^{\bullet}$ radicals upon its coordination to the V centre

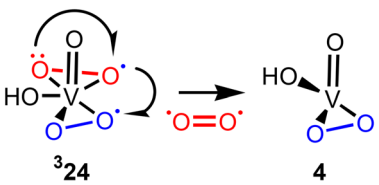

Fig. 8 Liberation of O_2 in complex ^{3}**24**.

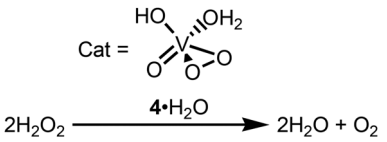

Scheme 10 Dismutation of H_2O_2 catalysed by the complex **4·H$_2$O**.

in the simple vanadate has been postulated as the reason for such low activity. However, to the best of our knowledge, no systematic studies aimed at supporting this assumption have been undertaken. In this article, the results of the detailed mechanistic study of HO$^{\bullet}$ formation in the vanadate/$H_2O_{2(aq)}$/MeCN system are reported.

This work resulted in two unexpected discoveries which finally shed light on this issue. First, the commonly accepted mechanism of the vanadium(v) catalysed oxidation of alkanes with H_2O_2 represented in the most general form by eqn (1) and (2) was revisited. *Another mechanism of HO$^{\bullet}$ generation (eqn (3)) based on the participation of a non-innocent ligand – which was not previously considered for the V activation of H_2O_2 toward homolysis – was found to be not only feasible but also more favourable than the conventional mechanism.*

$$HO\text{–}[V^{V}]\text{–}OOH + H_2O_2 \rightarrow HO\text{–}[V^{IV}]\text{–}O_2H_2 + HOO^{\bullet} \quad (1)$$

$$HO\text{–}[V^{IV}]\text{–}O_2H_2 \rightarrow H_2O\text{–}[V^{V}]{=}O + HO^{\bullet} \quad (2)$$

$$[V^{V}]\text{–}OOH \rightarrow [V^{V}]{=}O + HO^{\bullet} \quad (3)$$

This new mechanism starts with the formation of the hydroperoxo diperoxo complex [V(OOH)(OO)$_2$(H$_2$O)] **10·H$_2$O** upon several H_2O-for-H_2O_2 substitution and H^+-transfer steps – **10·H$_2$O** being the most stable catalytic form in the vanadate/$H_2O_{2(aq)}$/MeCN system – and includes simple monomolecular homolytic VO–OH bond cleavage in **10·H$_2$O** affording [V(=O)(OO)$_2$(H$_2$O)] **20·H$_2$O** and HO$^{\bullet}$ (Scheme 11). Despite the V atom being in its highest oxidation state in **10·H$_2$O**, the further oxidation of the catalyst may occur upon VO–OH bond cleavage due to the presence of the non-innocent peroxo ligand which is oxidized instead of the metal centre. The reaction product **20·H$_2$O**, thus, represents the V(v) species bearing one peroxyl

Open Access Article. Published on 22 May 2023. Downloaded on 1/22/2026 3:04:01 PM.
This article is licensed under a Creative Commons Attribution-NonCommercial 3.0 Unported Licence.

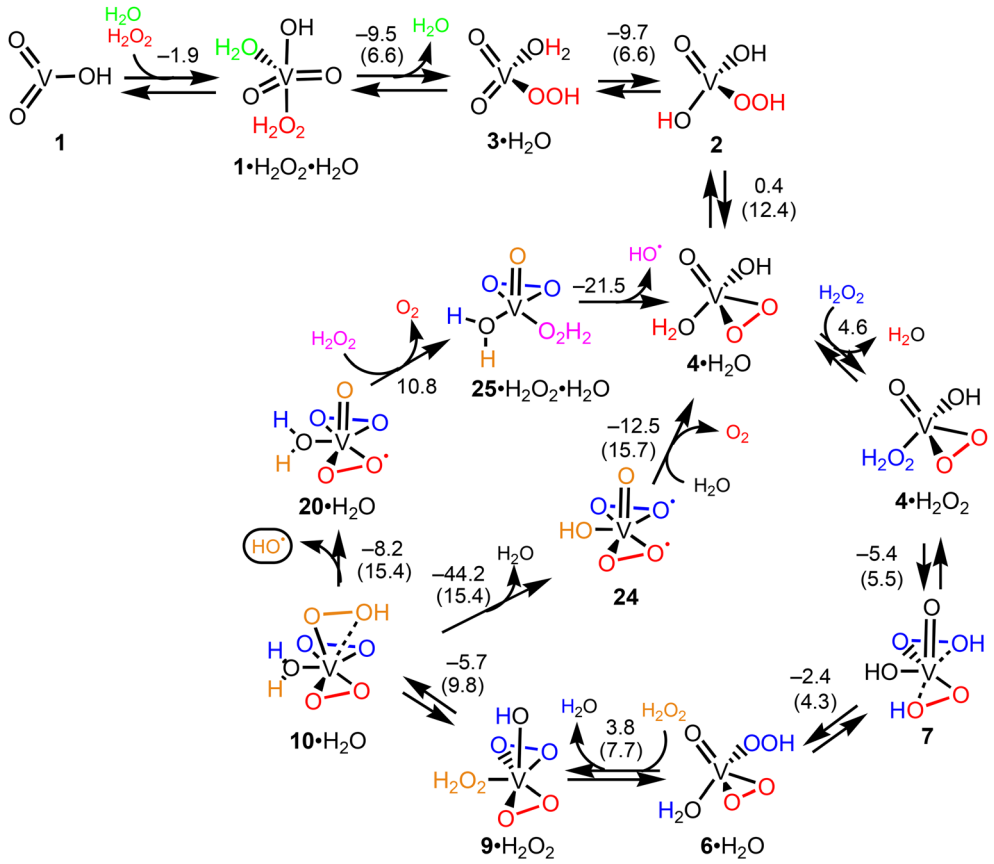

Scheme 11 Overall non-innocent ligand mechanism of HO˙ generation in the vanadate/$H_2O_{2(aq)}$/MeCN system and of the side reaction of H_2O_2 dismutation *via* complex **24** (reaction and activation (in parentheses) energies are indicated in terms of Gibbs free energies in kcal mol^{-1}).

anion-radical ligand $(OO)\cdot^{-}$, and the oxidation state of the vanadium is not altered. The VO–OH bond rupture in **10·H$_2$O** yields one HO˙ radical and one peroxyl anion-radical $(OO)^{\bullet-}$ which, being coordinated to the V centre, is quite stable. Such a stabilization of one of the products explains the tremendous thermodynamic activation of the OOH ligand in **10·H$_2$O**. Thus, the role of the non-innocent ligand in the generation of the HO˙ radicals from H_2O_2 is not restricted to the catalysts with the metals bearing the only one stable oxidation state, reported previously.[42–44] A similar mechanism is also applicable to catalysts based on the metals with variable oxidation states.

The calculations demonstrate that the overall activation barrier of HO˙ generation in the vanadate/$H_2O_{2(aq)}$/MeCN system (15.4 kcal mol^{-1}) is sufficiently low to permit efficient radical formation. *The second principal result of this work indicates that the low efficiency of the simple vanadate in the oxidation of alkanes is not related to insufficient activation of H_2O_2 by the V catalyst.* Instead, an easy capture of the generated HO˙ by the V atom decreases the effective concentration of HO˙ in the reaction mixture and, therefore, hampers the following oxidation of alkanes. This side reaction corresponds to the catalytic dismutation of H_2O_2 into O_2 and H_2O (Scheme 11).

The V atom in the complex **10·H$_2$O** is an efficient HO˙ radical trap because it has an unsaturated coordination sphere. Saturation of the coordination sphere in **10·H$_2$O** by a solvent molecule (*e.g.* H_2O) is not thermodynamically feasible (ΔG° = 5.2 kcal mol^{-1}). In contrast, the formation of **24** from **10·H$_2$O** is highly exergonic (ΔG° = −44.2 kcal mol^{-1}) and, additionally, the following O_2 elimination also has a negative ΔG° value (−12.5 kcal mol^{-1}).

Application of additives or V(v) complexes with various organic ligands often significantly improves the performance of the catalyst in comparison with the simple vanadate.[34,36,39] Taking into account the results of this work, it is possible to speculate that such an improvement is associated not with a higher activation of H_2O_2 by such catalysts but with the saturation of the V coordination sphere by organic ligands. For instance, the NMR spectroscopic studies showed that complexes **26a** and **26b** (Chart 1) are the predominant forms of the catalyst in solution of vanadate in the presence of H_2O_2 and PCAH.[36,39,65] These complexes have the saturated coordination sphere of the metal and, therefore, the V atom here cannot serve as an efficient HO˙ radical trap. This can explain the pronounced effect of the PCAH additive on the catalytic activity of vanadate in the alkane oxidation reaction. The verification of this hypothesis should be the subject of further investigations.

The role of the hydroperoxo V complexes as active catalytic species was revealed in the oxidation of halide anions with

 This journal is © The Royal Society of Chemistry 2023

Open Access Article. Published on 22 May 2023. Downloaded on 1/22/2026 3:04:01 PM.
This article is licensed under a Creative Commons Attribution-NonCommercial 3.0 Unported Licence.

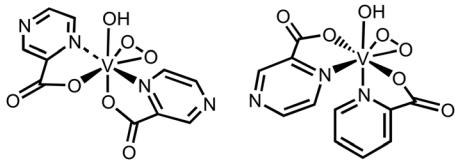

26a 26b

Chart 1

H_2O_2 catalysed by vanadium haloperoxidase enzymes or mimicking model complexes.[66–69] In this reaction, the OOH ligand undergoes two-electron reduction by the Hal^- anion while the latter is oxidized to the hypohalite anion $OHal^-$ which may be coordinated to the V atom (eqn (4)). The formed hypohalite oxidizes hydrogen peroxide to the molecular oxygen and water (eqn (5)), and the overall process corresponds to the dismutation of H_2O_2 (eqn. (4)–(7)).[67] In the case of the simple vanadate with an unsaturated coordination sphere, the generated $HO^\bullet$ radicals serve as such oxidizing species.

$$[V]\text{–}OOH + Hal^- \rightarrow HO\text{–}[V]\text{–}OHal^- \rightarrow [V]\text{–}O^- + HOHal \quad (4)$$

$$H_2O_2 + HOHal \rightarrow O_2 + Hal^- + H^+ + H_2O \quad (5)$$

$$[V]\text{–}O^- + H_2O_2 + H^+ \rightarrow [V]\text{–}OOH + H_2O \quad (6)$$

$$2H_2O_2 \rightarrow 2H_2O + O_2 \quad (7)$$

Data availability

Additional data may be found in the ESI‡ or could be requested from the authors.

Author contributions

MLK – conceptualization of the work, computational studies, writing and preparation of the manuscript. AJLP – conceptualization of the work, discussion of results, proof reading, and funding.

Conflicts of interest

The authors declare no conflict of interest.

Acknowledgements

This work was partially supported by the Fundação para a Ciência e a Tecnologia (FCT), Portugal, projects UIDB/00100/2020 and UIDP/00100/2020 of Centro de Química Estrutural and LA/P/0056/2020 of Institute of Molecular Sciences.

References

1 A. E. Shilov and G. B. Shul'pin, *Chem. Rev.*, 1997, **97**, 2879.
2 G. B. Shul'pin, *Mini-Rev. Org. Chem.*, 2009, **6**, 95.
3 R. H. Crabtree, *Chem. Rev.*, 1995, **95**, 987.
4 C. Jia, T. Kitamura and Y. Fujiwara, *Acc. Chem. Res.*, 2001, **34**, 633.
5 B. S. Lane and K. Burgess, *Chem. Rev.*, 2003, **103**, 2457.
6 G. Grigoropoulou, J. H. Clark and J. A. Elings, *Green Chem.*, 2003, **5**, 1.
7 *Alkane Functionalization*, ed. A. J. L. Pombeiro and M. F. C. Guedes da Silva, J. Wiley & Sons, Hoboken, NJ, USA, 2019.
8 J. A. Labinger, *J. Mol. Catal. A: Chem.*, 2004, **220**, 27.
9 B. L. Conley, W. J. Tenn III, K. J. H. Young, S. K. Ganesh, S. K. Meier, V. R. Ziatdinov, O. Mironov, J. Oxgaard, J. Gonzales, W. A. Goddard III and R. A. Periana, *J. Mol. Catal. A: Chem.*, 2006, **251**, 8.
10 J. Muzart, *J. Mol. Catal. A: Chem.*, 2007, **276**, 62.
11 M. M. Díaz-Requejo and P. J. Pérez, *Chem. Rev.*, 2008, **108**, 3379.
12 R. H. Crabtree, *Chem. Rev.*, 2010, **110**, 575.
13 J. A. L. da Silva, J. J. R. Fraústo da Silva and A. J. L. Pombeiro, *Coord. Chem. Rev.*, 2011, **255**, 2232.
14 *Vanadium catalysis*, ed. M. Sutradhar, J. A. L. da Silva and A. J. L. Pombeiro, Royal Society of Chemistry, Cambridge, UK, 2021.
15 R. R. Langeslay, D. M. Kaphan, C. L. Marshall, P. C. Stair, A. P. Sattelberger and M. Delferro, *Chem. Rev.*, 2019, **119**, 2128.
16 K. Nomura and S. Zhang, *Chem. Rev.*, 2011, **111**, 2342.
17 P. Schwendt, J. Tatiersky, L. Krivosudský and M. Šimuneková, *Coord. Chem. Rev.*, 2016, **318**, 135.
18 V. Conte, A. Coletti, B. Floris, G. Licini and C. Zonta, *Coord. Chem. Rev.*, 2011, **255**, 2165.
19 A. M. F. Phillips, H. Suo, M. F. C. Guedes da Silva, A. J. L. Pombeiro and W.-H. Sun, *Coord. Chem. Rev.*, 2020, **416**, 213332.
20 M. Kirihara, *Coord. Chem. Rev.*, 2011, **255**, 2281.
21 G. Licini, V. Conte, A. Coletti, M. Mba and C. Zonta, *Coord. Chem. Rev.*, 2011, **255**, 2345.
22 H. Hagen, J. Boersma and G. van Koten, *Chem. Soc. Rev.*, 2002, **31**, 357.
23 J.-Q. Wu and Y.-S. Li, *Coord. Chem. Rev.*, 2011, **255**, 2303.
24 H. Pellissier, *Coord. Chem. Rev.*, 2015, **284**, 93.
25 B. M. Weckhuysen and D. E. Keller, *Catal. Today*, 2003, **78**, 25.
26 N. F. Dummer, J. K. Bartley and G. J. Hutchings, *Adv. Catal.*, 2011, **54**, 189.
27 M. R. Maurya, A. Kumar and J. C. Pessoa, *Coord. Chem. Rev.*, 2011, **255**, 2315.
28 A. Chieregato, J. M. L. Nieto and F. Cavani, *Coord. Chem. Rev.*, 2015, **301–302**, 3.
29 J. C. Védrine, G. J. Hutchings and C. J. Kiely, *Catal. Today*, 2013, **217**, 57.
30 M. O. Guerrero-Pérez, *Catal. Today*, 2017, **285**, 226.

Open Access Article. Published on 22 May 2023. Downloaded on 1/22/2026 3:04:01 PM.
This article is licensed under a Creative Commons Attribution-NonCommercial 3.0 Unported Licence.

31 W. Chu, J. Luo, S. Paul, Y. Liu, A. Khodakov and E. Bordes, *Catal. Today*, 2017, **298**, 145.
32 N. Mizuno and K. Kamata, *Coord. Chem. Rev.*, 2011, **255**, 2358.
33 J. J. H. B. Sattler, J. Ruiz-Martinez, E. Santillan-Jimenez and B. M. Weckhuysen, *Chem. Rev.*, 2014, **114**, 10613.
34 I. Gryca, K. Czerwińska, B. Machura, A. Chrobok, L. S. Shul'pina, M. L. Kuznetsov, D. S. Nesterov, Y. N. Kozlov, A. J. L. Pombeiro, I. A. Varyan and G. B. Shul'pin, *Inorg. Chem.*, 2018, **57**, 1824.
35 H. Mimoun, L. Saussine, E. Daire, M. Postel, J. Fischer and R. Weiss, *J. Am. Chem. Soc.*, 1983, **105**, 3101.
36 M. V. Kirillova, M. L. Kuznetsov, V. B. Romakh, L. S. Shul'pina, J. J. R. Fraústo da Silva, A. J. L. Pombeiro and G. B. Shul'pin, *J. Catal.*, 2009, **267**, 140.
37 I. S. Fomenko, A. L. Gushchin, P. A. Abramov, M. N. Sokolov, L. S. Shul'pina, N. S. Ikonnikov, M. L. Kuznetsov, A. J. L. Pombeiro, Y. N. Kozlov and G. B. Shul'pin, *Catalysts*, 2019, **9**, 217.
38 M. Sutradhar, N. V. Shvydkiy, M. F. C. Guedes da Silva, M. V. Kirillova, Y. N. Kozlov, A. J. L. Pombeiro and G. B. Shul'pin, *Dalton Trans.*, 2013, **42**, 11791.
39 G. B. Shul'pin, Y. N. Kozlov, G. V. Nizova, G. Süss-Fink, S. Stanislas, A. Kitaygorodskiy and V. S. Kulikova, *J. Chem. Soc., Perkin Trans. 2*, 2001, 1351.
40 M. V. Kirillova, M. L. Kuznetsov, Y. N. Kozlov, L. S. Shul'pina, A. Kitaygorodskiy, A. J. L. Pombeiro and G. B. Shul'pin, *ACS Catal.*, 2011, **1**, 1511.
41 G. B. Shul'pin and G. Süss-Fink, *J. Chem. Soc., Perkin Trans. 2*, 1995, 1459.
42 M. L. Kuznetsov, Y. N. Kozlov, D. Mandelli, A. J. L. Pombeiro and G. B. Shul'pin, *Inorg. Chem.*, 2011, **50**, 3996.
43 A. S. Novikov, M. L. Kuznetsov, A. J. L. Pombeiro, N. A. Bokach and G. B. Shul'pin, *ACS Catal.*, 2013, **3**, 1195.
44 M. L. Kuznetsov, F. A. Teixeira, N. A. Bokach, A. J. L. Pombeiro and G. B. Shul'pin, *J. Catal.*, 2014, **313**, 135.
45 A. Burg, D. Shamir, I. Shusterman, H. Kornweitz and D. Meyerstein, *Chem. Commun.*, 2014, **50**, 13096.
46 A. Burg, I. Shusterman, H. Kornweitz and D. Meyerstein, *Dalton Trans.*, 2014, **43**, 9111.
47 A. G. DiPasquale, D. A. Hrovat and J. M. Mayer, *Organometallics*, 2006, **25**, 915.
48 A. G. DiPasquale, W. Kaminsky and J. M. Mayer, *J. Am. Chem. Soc.*, 2002, **124**, 14534.
49 C. Adamo and V. Barone, *J. Chem. Phys.*, 1999, **110**, 6158.
50 S. Grimme, S. Ehrlich and L. Goerigk, *J. Comput. Chem.*, 2011, **32**, 1456.
51 M. J. Frisch, G. W. Trucks, H. B. Schlegel, G. E. Scuseria, M. A. Robb, J. R. Cheeseman, G. Scalmani, V. Barone, B. Mennucci, G. A. Petersson, H. Nakatsuji, M. Caricato, X. Li, H. P. Hratchian, A. F. Izmaylov, J. Bloino, G. Zheng, J. L. Sonnenberg, M. Hada, M. Ehara, K. Toyota, R. Fukuda, J. Hasegawa, M. Ishida, T. Nakajima, Y. Honda, O. Kitao, H. Nakai, T. Vreven, J. A. Montgomery Jr., J. E. Peralta, F. Ogliaro, M. Bearpark, J. J. Heyd, E. Brothers, K. N. Kudin, V. N. Staroverov, R. Keith, J. Kobayashi, K. Normand, A. Raghavachari, J. C. Rendell, S. S. Burant, T. Iyengar, J. Tomasi, M. Cossi, N. Rega, J. M. Millam, M. Klene, J. E. Knox, J. B. Cross, V. Bakken, C. Adamo, J. Jaramillo, R. Gomperts, R. E. Stratmann, O. Yazyev, A. J. Austin, R. Cammi, C. Pomelli, J. W. Ochterski, R. L. Martin, K. Morokuma, V. G. Zakrzewski, G. A. Voth, P. Salvador, J. J. Dannenberg, S. Dapprich, A. D. Daniels, O. Farkas, J. B. Foresman, J. V. Ortiz, J. Cioslowski and D. J. Fox, *Gaussian 09, Rev. D.01*, Gaussian Inc., 2013.
52 M. Steinmetz and S. Grimme, *ChemistryOpen*, 2013, **2**, 115.
53 A. V. Marenich, C. J. Cramer and D. G. Truhlar, *J. Phys. Chem. B*, 2009, **113**, 6378.
54 L. Noodleman and D. A. Case, *Adv. Inorg. Chem.*, 1992, **38**, 423.
55 E. Ruiz, J. Cano, S. Alvarez and P. Alemany, *J. Comput. Chem.*, 1999, **20**, 1391.
56 E. Ruiz, A. Rodriguez-Fortea, J. Cano, S. Alvarez and P. Alemany, *J. Comput. Chem.*, 2003, **24**, 982.
57 C. Gonzalez and H. B. Schlegel, *J. Chem. Phys.*, 1991, **95**, 5853.
58 C. Gonzalez and H. B. Schlegel, *J. Chem. Phys.*, 1989, **90**, 2154.
59 C. Gonzalez and H. B. Schlegel, *J. Phys. Chem.*, 1990, **94**, 5523.
60 M. Bonchio, O. Bortolini, M. Carraro, V. Conte and S. Primon, *J. Inorg. Biochem.*, 2000, **80**, 191.
61 V. Conte, F. Di Furia and S. Moro, *J. Mol. Catal. A: Chem.*, 1997, **117**, 139.
62 V. Conte, F. Di Furia and S. Moro, *J. Mol. Catal. A: Chem.*, 1994, **94**, 323.
63 H. Schmidt, I. Andersson, D. Rehder and L. Pettersson, *Chem. – Eur. J.*, 2001, **7**, 251.
64 A. E. Gekhman, G. E. Amelichkina, N. I. Moiseeva, M. N. Vargaftik and I. I. Moiseev, *J. Mol. Catal. A: Chem.*, 2000, **162**, 111.
65 Y. N. Kozlov, V. B. Romakh, A. Kitaygorodskiy, P. Buglyó, G. Süss-Fink and G. B. Shul'pin, *J. Phys. Chem. A*, 2007, **111**, 7736.
66 B. J. Hamstra, G. J. Colpas and V. L. Pecoraro, *Inorg. Chem.*, 1998, **37**, 949.
67 G. J. Colpas, B. J. Hamstra, J. W. Kampf and V. L. Pecoraro, *J. Am. Chem. Soc.*, 1996, **118**, 3469.
68 A. Butler, *Coord. Chem. Rev.*, 1999, **187**, 17.
69 Z. Chen, *Coord. Chem. Rev.*, 2022, **457**, 214404.

This journal is © The Royal Society of Chemistry 2023